LIFELINE
EMERGENCY and SAFETY

Research Article

# Load-carrying capacity prediction method of box girder bridges based on diagnostic load testing

Meng-Di Yang[1], Xu Zheng[2,3,✉], Yu Zhou[4], Ting-Hua Yi[1]

**Cite this article:** Yang M - D, Zheng X, Zhou Y, et al. *Lifeline Emergency and Safety* 2026, **1**: 9660007. https://doi.org/10.26599/LLES.2025.9660007

**ABSTRACT:** Current bridge evaluation methods can give the bridge load-carrying capacity at the moment of field inspection and load testing. However, the evolution rule of the load-carrying capacity is also important since these testing cannot be implemented frequently. In order to accurately predict the bridge load-carrying capacity after load testing, this study first introduces the bridge initial load-carrying capacity calibration method by diagnostic load testing based on Chinese and US evaluation code. Then, the resistance degradation model is established to simulate the degradation path of bridge resistance based on the Gamma process. Combining the results of the initial resistance calibration and the degradation model, the time-varying bridge safety factor prediction method is proposed. Finally, the proposed method is verified through a load-carrying capacity prediction example of prestressed concrete continuous box girder bridge, and the results of the safety factor prediction in the unfavorable cross sections is given combined with diagnostic load test data. The outcome of this paper can provide a basis for management decisions such as bridge reinforcement, demolition, and replacement after bridge load testing.

**KEYWORDS:** Box girder bridge; resistance degradation model; load-carrying capacity evaluation; load testing; performance prediction

## 1 Introduction

Due to the coupled effects of material aging, environmental erosion and cyclic loading, the load-carrying capacity of in-service bridges will gradually decreases with the increase of service time[1-4]. Taking the in-service bridges in the United States as an example, there were approximately 56,000 bridges with structural deficiencies, accounting for about 9.1% of the total number of bridges. In recent years, although maintenance and repair have been carried out on such bridges both domestically and internationally, the collapse events still occur intermittently. To prevent the economic losses and catastrophic consequences caused by sudden bridge collapses, reliable evaluation of the load-carrying capacity of in-service bridges has become an urgent task in the field of bridge research. Box girder bridges, due to their advantages such as high lateral torsional stiffness and reasonable overall load-carrying capacity, play a significant role in highway transportation. Therefore, research focusing on prestressed concrete box girder bridges is of profound significance.

There are two major types of bridge load-carrying capacity evaluation methods: theoretical analysis methods and load testing methods. The load testing[5-6] methods were first applied in the aviation field, later gradually being used in the fields of building structures and bridges. Proof load testing[7-9] is a method that applies target proof loads to the bridge to directly demonstrate the load-carrying capacity. However, the implementation of proof load testing always require the layout of a large number of sensors and renting loading trucks, cannot meet the growing demands for bridge evaluation. Therefore, another load testing method, known as diagnostic load testing[10-13], has begun to gradually gain attention, as this method can establish the relationship between the actual behavior of bridges and analytical model. The current mainstream approach is to combine the results of diagnostic load testing with theoretical analysis methods. Theoretical analysis is a method that judges the bridge's load-carrying capacity by comparing the unfavorable load effects with the corrected resistance, and the resistance can be corrected through material laboratory test, field inspection and nondestructive testing. When the bridge's load-carrying capacity cannot be determined through theoretical analysis, refined analytical model, diagnostic load testing and field traffic investigation can be conducted to further exploit bridge safety reserves.

To reasonably predict the load-carrying capacity after a period of bridge evaluation, the resistance degradation rule of in-service bridges has attracted more attention in the field of bridge engineering. Based on the mechanism of bridge disease, researchers seek a resistance degradation model that can match the actual bridge degradation process. In the early phase, most researchers used deterministic degradation function to describe the resistance degradation process. For example, Mori et. al[14] proposed to use power function to express the resistance

[1] School of Civil Engineering, Dalian University of Technology, Dalian 116023, China. [2] School of Civil and Transportation Engineering, Beijing University of Civil Engineering and Architecture, Beijing 102616, China. [3] Key Laboratory of Damage Diagnosis for Engineering Structures of Hunan Province, Hunan University, Changsha 410082, China. [4] School of Civil Engineering, Anhui Jianzhu University, Hefei 230601, China.

✉ Corresponding author. E-mail: zhengxu@bucea.edu.cn

Received: November 4, 2024; Revised: December 3, 2024; Accepted: January 8, 2026

degradation process. But this model did not take into account the stochastic nature of the degradation process, so Enright et. al[15] added a zero-mean stochastic process to establish a new model of degradation. Thereafter Bhattacharya et. al[16] changed the model to a derivative form by taking into account the fact that the degradation of the resistances is a monotonically declining process. Although this model avoids the possibility of resistance increasing with time, it is difficult to implement in practical engineering because it involves additional parameters and is difficult to calibrate the experimental data. Therefore, the current mainstream method is to use a stochastic process function to simulate the bridge resistance degradation process. The commonly used stochastic processes include Wiener process, Gamma process and Inverse Gaussian (IG) process. Xu et al.[17] and Xu et al.[18] considered obtaining reliability estimates based on the Wiener process to achieve the prediction of the remaining useful life of batteries. Peihua Jiang[19] studied the Wiener constant-stress accelerated degradation model with random drift parameter and fixed diffusion parameter, which can be used to evaluate the reliability of products. Yang et al.[20] established a Gamma stochastic process degradation model considering the spatial degradation of resistance and proposed a new method for evaluating the reliability of aging structures. Based on the resistance degradation model of Gamma stochastic processes, Li et al.[21] established a time-varying reliability analysis framework considering stochastic processes. Rodríguez-Picón et al.[22] described the drift of the degradation process by integrating multiple hazard rate functions in the IG process and analyzed the degradation processes of two case studies. Based on IG stochastic process, Peng et al.[23] proposed a theoretical framework for updating the IG stochastic degradation process model by Bayesian principle.

The current load-carrying capacity evaluation methods based on load testing can only evaluate the load-carrying capacity at a certain moment, but the bridge is still required for a long period of service after the load testing. In order to grasp the long-term evolution rule of bridge load-carrying capacity, it is essential to develop a method of load-carrying capacity prediction based on the evaluation results in certain moment. This paper proposed a rapid evaluation method of load-carrying capacity of box girder bridge based on influence line identification, virtual loading and degradation modeling, and then established an evaluation process consisting of the initial resistance calibration, the resistance degradation process simulation and the time-varying bridge safety factor prediction. At the end of the paper, the validity of the method is verified by a prestressed concrete continuous box girder bridge load-carrying capacity prediction example. The outcome of this paper can realize the load-carrying capacity prediction of in-service bridges in the future stage, which can provide the basis for the management decision of bridge load limitation, maintenance and reinforcement after bridge load testing.

Based on this, the main contributions and novelties of this paper are summarized as follows:

- A method for correcting the initial resistance of box girder bridges based on diagnostic load testing is proposed. It addresses the drawbacks of traditional load tests, including high cost and operational complexity, and facilitates rapid resistance calibration.
- A resistance degradation model of box girder bridges based on the Gamma stochastic process is established, thus enabling the prediction of long-term load-carrying capacity evolution.
- A formula for calculating the safety factor of the load - carrying capacity of box girder bridges is constructed, thus providing support for timely decision-making on bridge load limitation, maintenance, and reinforcement.

## 2 Initial resistance calibration based on bridge evaluation codes

This chapter will introduce how to achieve the initial calibration of bridges resistance based on the results of diagnostic load tests, in accordance with the American Code “the Manual for Bridge Evaluation”[24] and the Chinese Code “Specification for Inspection and Evaluation of Load-bearing Capacity of Highway Bridges” (JTG/T J21)[25].

### 2.1 Initial resistance calibration method in American bridge evaluation codes

The American Association of State Highway and Transportation Officials (AASHTO)[24] stipulates that the carrying capacity of bridges should be determined through theoretical analysis in combination with field inspection and material testing. The objective of analysis is to determine the rating factor RF, the magnitude of RF can reflect the safety reserve of live load capacity. $\mathrm{RF} \succ 1$ proves that the bridge satisfies the capacity of the target live load. The rating factor based on load-resistance factor evaluation method can be determined by Eq. (1).

$$\mathrm{RF} = \frac{C - \gamma_{\mathrm{DC}}\mathrm{DC} - \gamma_{\mathrm{DW}}\mathrm{DW} \pm \gamma_{\mathrm{P}}P}{\gamma_{\mathrm{LL}}(\mathrm{LL}+\mathrm{IM})} \tag{1}$$

where $C$ is the load-carrying capacity; DC is the dead load effect due to structural components and attachments; DW is the dead load effect due to wearing surface and utilities; $P$ is permanent loads other than dead loads; $\gamma_{\mathrm{DC}}$ is theload resistance factor design (LRFD) load factor for structural components and attachments; $\gamma_{\mathrm{DW}}$ is the LRFD load factor for wearing surfaces and utilities; $\gamma_{\mathrm{P}}$ is the LRFD load factor for permanent loads other than dead loads; $\gamma_{\mathrm{LL}}$ is the evaluation live load factor; LL is live load effect; IM is the dynamic load allowance.

To evaluate the difference between the theoretical response and the measured response after diagnostic load testing, an adjustment factor $K$ was introduced[24] to modify the rating factor. After the implementation of diagnostic load testing, the strain time history of bridge key cross-sections can be measured. The rating factor is then modified through adjustment factor $K$ according to Eq. (2).

$$\mathrm{RF}_{\mathrm{T}} = \mathrm{RF}_{\mathrm{C}}K \tag{2}$$

where, $\mathrm{RF}_{\mathrm{T}}$ is the load-rating factor for the live-load capacity based on the load test result; $\mathrm{RF}_{\mathrm{C}}$ is the rating factor based on calculations made prior to the diagnostic load test. $K$ is an adjustment factor resulting from the comparison of measured test behavior with the analytical model, which can be calculated by Eq.(3).

$$K = 1 + K_{\mathrm{a}}K_{\mathrm{b}} \tag{3}$$

Where $K_{\mathrm{a}}$ is the benefit derived from the load test, which can be determined by Eq.(4); $K_{\mathrm{b}}$ represents the expected level of test benefit at the rating load level, with values ranging between 0 and 1.0[24].

$$K_{\mathrm{a}} = \frac{\varepsilon_{\mathrm{c}}}{\varepsilon_{\mathrm{T}}} - 1 \tag{4}$$

where $\varepsilon_c$ is the corresponding calculated strain generated by the position of the test vehicle on the bridge, and $\varepsilon_T$ is the maximum member strain measured during load test.

### 2.2 Initial resistance calibration method in Chinese bridge evaluation codes

According to the Chinese code[25], the load-carrying capacity of a bridge should be determined through theoretical analysis in combination with materials testing, defects inspection, parameter identification and load testing. The objective of the theoretical analysis is to determine the relationship between the load effect and the resistance of the bridge in Eq. (5):

$$\gamma_0 S \leqslant R(f_d, \xi_c a_{dc}, \xi_s a_{ds}) Z(1-\xi_e) \tag{5}$$

where $\gamma_0$ is the structural importance coefficient; $S$ is the load effect function; $R(\cdot)$ is the resistance function; $f_d$ is the design value of material strength; $\xi_c$ is the section-reduction coefficient for reinforced concrete structures; $\xi_s$ is section-reduction coefficient for reinforcing steel; $a_{dc}$ is the value of the geometric parameter of the member concrete; $a_{ds}$ is the value of the geometric parameter of the member reinforcement; $\xi_e$ is the deterioration coefficient of load-bearing capacity; $Z$ is the comprehensive modification of bridge load-bearing capacity. By comprehensively considering the bridge defect condition, concrete strength, and structure natural frequency parameters, the overall condition of the bridge is reflected, and then the value range of $Z$ is obtained. When the bearing capacity cannot be evaluated through the calculation analysis, the load test should be carried out to re-determine the value of $Z$.

Although the above methods are commonly used in the evaluation of bridge load-carrying capacity, there are shortcomings such as high cost and large amount of engineering work in obtaining $Z$, which cannot realize the rapid evaluation of bridge load-carrying capacity. In order to solve these problems, this paper adopts a rapid evaluation method of bridge load-carrying capacity based on influence line identification and virtual loading.

The accurate and effective field test data is the basis for recognizing the bridge influence lines (BILs). The axle distance, axle weight and real-time position of the test truck are obtained through the test of truck parameters, and these parameters are used to construct the information matrix of calibration truck $\boldsymbol{L}$. The bridge response time course is obtained through the bridge response test during truck passage, and the column vector of bridge response $\boldsymbol{R}$ is constructed. According to Eq. (6), the problem of BILs can be transformed into solving the system of linear equations and extracting the column vector of influence coefficients $\boldsymbol{\varphi}$.

$$\boldsymbol{R} = \boldsymbol{L\varphi} \tag{6}$$

When the $i$th load $P_i$ acts on the bridge, according to the influence coefficient $\varphi_i^j$ of the measuring point $j$ corresponding to the load at the position $i$ of the bridge, the response $S_v$ of the measuring point can be predicted as shown in Eq. (7).

$$S_v = \sum_{i=1}^{n} P_i \varphi_i \tag{7}$$

In order to reflect the difference between the real and theoretical conditions of the bridge, the virtual loading calibration coefficient should be introduced as in Eq. (8).

$$\eta_v = \frac{S_v}{S_s} \tag{8}$$

where, $S_v$ is the displacement or strain value under control load or platoon load obtained by virtual loading; $S_s$ is the theoretical calculated displacement or strain value of the main measuring point under the corresponding virtual load.

The modification coefficient for rapid evaluation of bridge load-carrying capacity $Z_v$ based on virtual loading calibration coefficient to determine. The specific method for determining its value is shown in Table 1.

**Table 1 The modification coefficient for rapid evaluation of bridge load-carrying capacity $Z_v$.**

| $\eta$ | $Z_v$ | $\eta$ | $Z_v$ |
|---|---|---|---|
| ⩽0.4 | 1.30 | 0.8 | 1.00 |
| 0.5 | 1.20 | 0.9 | 0.90 |
| 0.6 | 1.15 | 1.0 | 0.80 |
| 0.7 | 1.10 | — | — |

Based on the rapid evaluation method proposed above, the load-carrying capacity evaluation method in the Chinese code[25] can be optimized by replacing $Z_v$ with $Z$.

## 3 Load-carrying capacity prediction based on degradation model

Stochastic processes are widely used in the stochastic modeling of various material degradation problems due to their good applicability to uncertain problems. The commonly used stochastic processes include Wiener process, Gamma process, and IG process. Due to the randomness and time-varying variability of bridge load-carrying capacity degradation process, how to select a suitable stochastic process model is a hot topic in bridge research. Based on the factors influencing the resistance degradation of box girder bridges and the actual bridge degradation process, this chapter compares and analyzes the adaptability of various stochastic processes to such degradation.

### 3.1 Degradation mechanism of box-girder bridge resistance

The resistance influence factors of box girder bridge can be divided into load, environment and material internal factors, among which load factors will not only directly affect the safety of the structure, but also cause damage to the structure, including static cumulative damage and dynamic cumulative damage. The environmental factors are the most important factors affecting the bridge resistance. The main injuries are steel corrosion, concrete corrosion and section cracking caused by chloride ion, carbon dioxide and sulfate corrosion. The slow internal chemical reactions between some active materials and other components can also cause irreversible damage to the bridge.

Generally, the analytic hierarchy process is used to extract the main resistance influence factors of bridges for subsequent analysis. The factors that need to be considered are generally chlorine ion erosion, steel corrosion, concrete carbonization, section cracking, concrete strength changes, and section geometric damage. In the early stage of box girder bridge service, the main factors of resistance degradation are concrete carbonation and steel corrosion caused by carbon dioxide and chloride ion erosion. With the increase of service time of box girder bridge, cracks begin to appear on the surface of concrete, which accelerates the corrosion of steel bars. The coupling effect of various factors at different stages leads to the resistance degradation process is not a stable process.

### 3.2 Establishment of box-girder bridge resistance degradation model

At present, the mainstream algorithm is to regard the resistance degradation process as a non-stationary random process. For non-stationary stochastic processes, Wiener process model, Gamma stochastic process model and IG stochastic process model are commonly used. A notable feature of the Wiener process is that its paths are not necessarily monotonic, which makes it irrelevant in many degradation simulations, including the resistance degradation process. Resistance degradation is a monotonically increasing process, and the most commonly used model is the Gamma process. In recent years, some scholars have argued that the IG process[26] can simulate a broader range of degradation data, but the IG distribution is unstable, and the initial IG stochastic process degradation model is not compatible with the bridge degradation process. Without sufficient actual inspection data, it is difficult to simulate the resistance degradation process of bridges. Therefore, this chapter selected the Gamma process to establish a resistance degradation model for box girder bridges.

The Gamma process[27] is a continuous-time stochastic process with random independent and non-negative increments. This characteristic renders it highly suitable for simulating the sequences of small incremental damage accumulation as time progresses. This approach aims to more accurately reflect the random nature of the performance degradation of box girder bridges, the formula of resistance degradation coefficient proposed by Li et. al[21] is used.

$$G(t) = 1 - \sum_{i=1}^{n} \hat{d}(t_i) \cdot \varepsilon(t_i) \tag{9}$$

where $\hat{d}(t_i)$ is the average degradation over time from $t_{i-1}$ to $t_i$, can be expressed as

$$\hat{d}(t_i) = k t_i^m \Delta t \tag{10}$$

where $k$ and $m$ represent the scale parameters and shape parameters of $\hat{d}(t_i)$ respectively; $\Delta t$ represents the time interval; $\varepsilon(t_i)$ is an independent random variable subject to gamma distribution, whose shape parameters and scale parameters are respectively

$$\begin{cases} \alpha(t_i) = \hat{d}(t_i)/\xi \\ \lambda(t_i) = \xi/\hat{d}(t_i) \end{cases} \tag{11}$$

The mean and the standard deviation of the degradation function are

$$\begin{cases} \mu_{G(t)} = 1 - \dfrac{k}{m+1} t^{m+1} \\ \sigma_{G(t)} = \sqrt{\dfrac{k\xi}{m+1} t^{m+1}} \end{cases} \tag{12}$$

The resistance degradation model based on gamma process includes three key parameters: $m, k, \xi$.

### 3.3 Load-carrying capacity prediction method

At present, the evaluation of bridge load-carrying capacity can only focus on the operation safety of in-service bridges at a particular point in time, but the performance of the bridge changes with time, so the evolution rule of load-carrying capacity after evaluation is equally important. In order to accurately predict the load-carrying capacity of the bridge after the load testing, this paper continues the concept and method of the Chinese code[25], and the load-carrying capacity evaluation formula is further optimized with the help of resistance degradation model. Referring to the formula of evaluation factor *RF* in the American code[24], the time-dependent safety factor formula for box girder bridges is obtained as shown in Eq. (13).

$$w = \frac{\gamma_0 \left[ \sum_{i=1}^{n} \gamma_{G,i} G_{i,k} + \gamma_Q (1+\mu) Q_k \right]}{G(t) R(f_d, \xi_c a_{dc}, \xi_s a_{ds}) Z_v (1-\xi_e)} \tag{13}$$

where $\gamma_{G,i}$ and $G_{i,k}$ are the partition coefficients for the $i$th permanent action and the assessment standard value of the permanent action effect, respectively; $\gamma_Q$, $\mu$, and $Q_k$ are the partition coefficients for the vehicle load effect, the impact coefficient, and the assessment standard value, respectively.

The magnitude of $w$ can reflect the safety reserve of load capacity. $w \prec 1$ proves that the bridge load-carrying capacity to meet the requirements.

## 4 Illustrative example for load-carrying capacity prediction

Combined with the above mentioned rapid evaluation method of bridge load-carrying capacity, this chapter takes a four-span double-beam bridge as an example for illustration.

### 4.1 Basic situation of the box girder bridge

The tested bridge is a prestressed concrete continuous box girder bridge, which is a separate double-span bridge with a single span width of 15.75 m. The bridge deck pavement adopts asphalt concrete pavement. The top of the box girder is equipped with a one-way 2% transverse slope, and the bottom plate is equipped with a flat slope. The actual condition of the bridge to be tested is shown in Figure 1.

**Fig. 1 Actual photo of the South span of the tested bridge. Photograph by Yu Zhou 2023.**

The upper part of the main bridge is a four-span, three-lane prestressed concrete variable-section continuous box girder. The main girder is made of C50 concrete. The top beam of the main pier is 4.8 m high, the thickness of the web is 0.7 m, the thickness of the roof is 0.28 m, and the thickness of the floor is 0.6 m. The height of the main beam and the thickness of the bottom plate are changed by quadratic parabola, the height of the middle span beam becomes 2 m, and the thickness of the bottom plate becomes 0.35 m. The box girder flange plate cantilever is 3.5 m long.

The box girder is a three-way prestressed structure, the longitudinal prestressed steel strands of the roof and floor adopt $\varphi^s 15.2$ steel strands, the tension control stress is 1,395 MPa, and the transverse prestressed steel strands adopts $\varphi^s15.2$ steel strands. The vertical prestress is finished rolling threaded steel bar. The prestressed steel strand adopts low-relaxation high-strength steel strand with standard value of tensile strength $f_{PK}=1,860$ MPa, nominal diameter $d$=15.2 mm. The concrete bulk density of the main bridge is 26 kN/m³. The cross-section geometry and reinforcement layout diagram of the tested bridge at mid-span cross-section, cross-section at $L$/4 and $h$/2 from the support are shown in Figure 2. $L$ is bridge span and $h$ is height of support section.

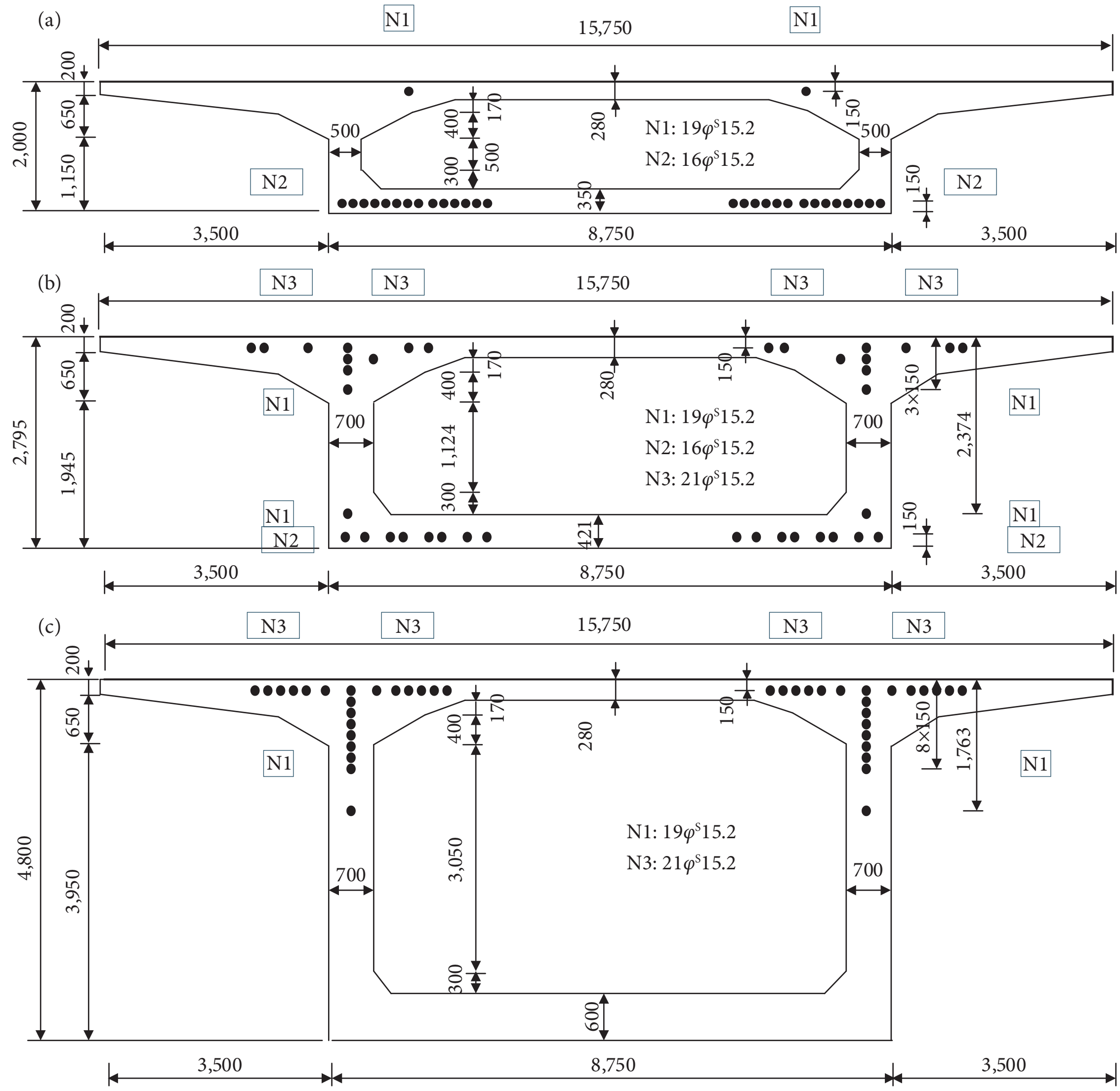


**Fig. 2 The tested bridge cross-section size and steel strand: (a) cross-section diagram at mid-span; (b) cross-section diagram at $L$/4; (c) cross-section diagram at $h$/2 from the support. (Unit: mm)**

## 4.2 Field test conditions

To comprehensively evaluate the performance of the tested bridge, a load test containing two loading conditions was carried out. In load case 1, a single loaded vehicle passed through each lane of the test bridge at a crawling speed, and was loaded twice in each lane to test the influence surface. In load case 2, three loading vehicles are running side by side, with the positioning system placed on the middle loaded vehicle. The field diagram of the staff conducting the load test is shown in Figure 3. By combining the corresponding data of each measuring point with the positioning data of the loaded vehicles, the influence lines of each measuring point were identified. The influence surface is the extension of the influence line, and according to the literature[28], the results of calculations using the influence surface are more accurate.

**Fig. 3 Field implementation of load test.**

### 4.3 Initial resistance calibration

Based on the key points for checking and calculating specified in the standards[25], the shearing force at a distance of $h/2$ from the center of the support, as well as the bending moment at the midspan and at the points one-fourth of the span length, are separately verified. The calculation of the bridge shearing force and bending moment is carried out in accordance with the "Specifications for Design of Highway Reinforced Concrete and Prestressed Concrete Bridges and Culverts" (JTG 3362-2018) [29].

For the box-shaped cross-section, a cross-section transformation is performed, where the effective width $b_f$ of the compressed flange of I-section after equivalent does not change, the equivalent thickness is $h_f$, and the web thickness is $2b$.

The flexural capacity of the prestressed box-shaped cross-section can be obtained from the equivalent I-section. First, it is necessary to determine the category of the I-section, and the method for this judgment is as Eq. (14).

$$\begin{cases} \xi_s f_{pd} A_p \leqslant \xi_c f_{cd} b_f h_f + \xi_s \left(f'_{pd} - \sigma'_{po}\right) A'_p \\ \xi_s f_{pd} A_p \geqslant \xi_c f_{cd} b_f h_f + \xi_s \left(f'_{pd} - \sigma'_{po}\right) A'_p \end{cases} \tag{14}$$

The bending moment calculation model for the first type of T-section is

$$R = \xi_c f_{cd} b_f x \left(h_0 - \frac{x}{2}\right) + \xi_s \left(f'_{pd} - \sigma'_{p0}\right) A'_p \left(h_0 - a'_p\right) \tag{15}$$

$$x = \frac{\xi_s f_{pd} A_p - \xi_s \left(f'_{pd} - \sigma'_{p0}\right) A'_p}{\xi_c f_{cd} b_f} \tag{16}$$

The bending moment calculation model for the second type of T-section is

$$\begin{aligned} R = {} & \xi_c f_{cd} \left[ bx \left(h_0 - \frac{x}{2}\right) + \left(b_f - b\right) h_f \left(h_0 - \frac{h_f}{2}\right)\right] \\ & + \xi_s \left(f'_{pd} - \sigma'_{p0}\right) A'_p \left(h_0 - a'_p\right) \end{aligned} \tag{17}$$

$$x = \frac{\xi_s f_{pd} A_p - \xi_s \left(f'_{pd} - \sigma'_{p0}\right) A'_p - \xi_c f_{cd} h_f \left(b_f - 2b\right)}{\xi_c f_{cd} b} \tag{18}$$

where $f_{cd}$ is the design value of axial compressive strength of the concrete; $f_{pd}$ and $f'_{pd}$ are the design value of the tensile strength and compressive strength of longitudinal prestressed reinforcement; $A_p$ and $A'_p$ are the cross-sectional area of the longitudinal prestressed reinforcement in the tension zone and compression zone; $b$ is the web width of the T-shaped cross-section; $h_0$ is the effective height of the section; $a'_p$ is the distance from the edge of the compression zone for the combined action point of the prestressed reinforcement; $\sigma'_{p0}$ is the stress in the prestressed reinforcement at the point where the normal stress of the concrete at the center of the compression zone is zero.

The shear capacity of the oblique section is calculated according to Eqs. (19)–(21).

$$V = V_{cs} + V_{pb} \tag{19}$$

$$\begin{aligned} V_{cs} = {} & 0.45 \times 10^{-3} \alpha_1 \alpha_2 \alpha_3 b \xi_c h_0 \\ & \sqrt{\left(2 + 0.6P\right) \sqrt{\xi_c f_{cu,k}} \left(\rho_{sv} \xi_s f_{sv} + 0.6 \rho_{pv} \xi_s f_{pv}\right)} \end{aligned} \tag{20}$$

$$V_{pb} = 0.75 \times 10^{-3} \xi_s f_{pd} \sum A_{pb} \sin \theta_p \tag{21}$$

where $V_{cs}$ is the design value of the combined shear capacity of concrete and stirrups within the oblique section; $V_{pb}$ is the design value of the shear capacity of the internal prestressed bent-up reinforcement intersecting the oblique section; $P$ is the reinforcement ratio of the longitudinal tensile reinforcement within the oblique section; $f_{cu,k}$ is the standard compressive strength of a concrete cube with a side length of 150 mm; $\rho_{sv}$ and $\rho_{pv}$ are the reinforcement ratios of the stirrups and vertical prestressed reinforcement within the oblique section; $f_{sv}$ and $f_{pv}$ are the design tensile strengths of the stirrups and vertical prestressed reinforcement; $A_{pb}$ is the cross-sectional areas of the internal prestressed bent-up reinforcement; $\theta_p$ is the angles between the tangent lines of the internal prestressed bent-up reinforcement and the horizontal line; $\alpha_1$, $\alpha_2$ and $\alpha_3$ are the influence coefficient for hogging moments, the prestressing enhancement coefficient, and the influence coefficient of the compressive flange, respectively. The definitive procedures for determining these coefficients are provided in the literature[29]. The initial resistance results calculated are shown in Table 2.

**Table 2 Calculated initial resistance of the tested box girder bridge.**

| Position | Checking parameters | Initial resistance $R_0$ | Revised resistance $R'_0$ |
|---|---|---|---|
| Midspan | Bending moment (N·m) | $1.33 \times 10^8$ | $1.57 \times 10^8$ |
| $L/4$ | Bending moment (N·m) | $1.66 \times 10^8$ | $1.96 \times 10^8$ |
| $h/2$ from the support | Shearing force (N) | $3.43 \times 10^7$ | $4.05 \times 10^7$ |

Note: $L$ bridge span; $h$ height of support section.

First, a preliminary correction of the resistance is made based on appearance inspection. Considering that the bridge is a new bridge, the cross-sectional reduction coefficient $\xi_c$ and $\xi_s$ is taken as 1. According to the literature[28], based on the comparison between the field test BIS and the finite element model of the bridge, considering the load effect, the virtual loading calibration coefficient $\eta$ is calculated to be 0.54. By referring to Table 1, the modification coefficient for rapid evaluation of bridge load-carrying capacity $Z_v$ is determined to be 1.18. The resistance after calibration is presented in Table 2.

### 4.4 Load-carrying capacity prediction result

To accurately predict the load-carrying capacity of the box girder bridge after the load test, this paper established a resistance degradation initial model based on the Gamma stochastic process. This degradation model mainly includes three key parameters: $k, m, \xi$. Suggestions on the values of the above parameters have been given in similar studies[21,30]. In this paper, $k = 0.00005$, $m = 1.5$, $\xi = 0.01$ are selected for subsequent analysis. Figure 4(a) and Figure 4(b) show the simulation results of the resistance

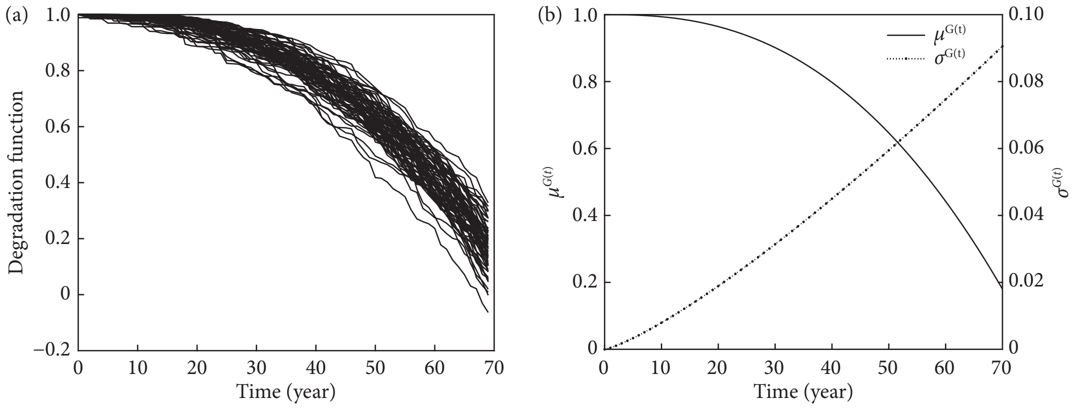


**Fig. 4 Degradation curve of bridge resistance: (a) simulation of resistance degradation process; (b) time-varying curves of mean value and covariance of resistance degradation coefficient.**

deterioration process and the characteristic values of the resistance deterioration coefficient over time, respectively. Each curve in Figure 4(a) represents a possible deterioration path.

To simplify the calculation, we approximately take the resistance deterioration coefficient as the mean value of the deterioration coefficient. Based on Eq. (22)[31], we can predict the degradation of resistance in future stages, and the time-varying curve of resistance is shown in Figure 5(a). It can be observed from the figure that the rate of decline in the three curves increases as the service time grows, which is related to the different main factors affecting the degradation of prestressed concrete bridges. The tested bridge will experience varying degrees of disease at different stages of its service life, and the cumulative accumulation of these diseases leads to different rates of performance degradation. Figure 5(a) further verifies that the resistance degradation process is a non-stationary stochastic process.

$$R(t) = G(t) R'_0 \tag{22}$$

On the basis of obtaining the time-varying resistance of the tested bridge, an accurate assessment of its safety during the service life requires consideration of the load effects under the most unfavorable load combinations. According to the provisions of Chinese code[25], when calculating the load effects of the tested bridge, the design load and the partition coefficients should be used. Then, according to Eq. (13), the safety factor of the tested bridge can be calculated and its time-varying curve is shown in Figure 5(b). Similar to Figure 5(a), the safety factor also exhibits a non-stationary process over time. After 50 years of service, there is a significant increase in the trend. By comparing the safety factor curves of the three sections, it is found that the safety factor of the quarter-point section is always less than 1 compared to the other two sections, indicating that there is a larger margin of load-carrying capacity. The other two sections reach the critical point around 45 and 50 years, respectively. After the bridge reaches the critical point, its reliability will be lower than the design target. However, this does not mean that the tested bridge has already failed. In the initial design stage of the bridge, a certain level of safety redundancy is usually set. Even after about 50 years of service, the reliability of the bridge may no longer meet the requirements of the design target, but it may still be able to maintain its basic functions. Moreover, the evaluation methods stipulated by Chinese codes are relatively conservative. Based on this, we cannot simply regard the situation where the safety factor is greater than 1 as the failure of the bridge. However, to ensure safety of the bridge throughout its entire service life, it is necessary to evaluate the load-carrying capacity of the bridge before the critical point and determine whether measures such as reinforcement, maintenance, or restrictions on heavy vehicles are required.

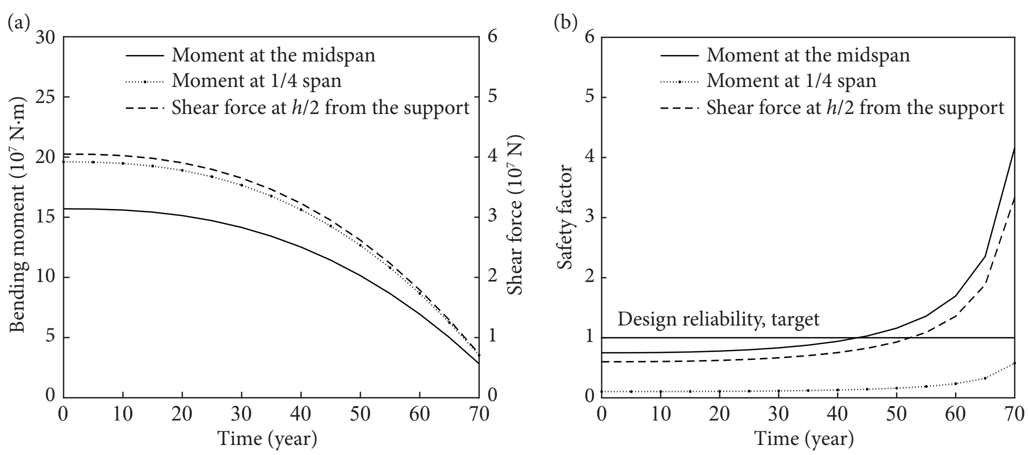


**Fig. 5 Time-varying prediction of load-carrying capacity: (a) time-varying diagram of bridge resistance; (b) time-varying curves of the safety factor.**

## 5 Conclusion

To address the issue of not being able to grasp the long-term evolution of the load-carrying capacity of in-service box girder bridges, this paper proposes a rapid assessment method for the load-carrying capacity of box girder bridges, which introduces the methods of influence line virtual loading and Gamma stochastic process. An assessment process consisting of initial resistance calibration, resistance degradation process simulation, and prediction of load-carrying capacity safety factor has been established. The effectiveness of this method is verified through a case of predicting the load-carrying capacity of a prestressed concrete continuous box girder bridge, and the main conclusions are as follows:

(1) By referring to American and Chinese codes, this paper introduces several commonly load-carrying capacity evaluation methods and provides the basic formulas for the theoretical analysis method. Combined with the rapid load test method, a method for correcting the initial resistance of box girder bridges based on diagnostic load testing is established, which can effectively tap the margin of load-carrying capacity and improve the accuracy of load-carrying capacity evaluation.

(2) In view of the shortcomings of deterministic degradation models in accurately describing the randomness and variability of the resistance degradation process of box girder bridge components, this paper introduces a resistance degradation model of box girder bridges based on the Gamma random process, and proposes a bridge load-carrying capacity prediction method. This method can provide support for operational decisions such as reinforcement, replacement, and demolition.

(3) Taking a prestressed concrete box girder bridge an example, this paper predicts the load-carrying capacity of the tested bridge during its service life. The case results show that the time-dependent safety factor based on the quarter-point section indicates that the tested bridge meets the designed reliability, while the safety factor time-dependent curves for the midspan section and the section at $h/2$ from the support indicate that after around 50 years' service, the reliability of the bridge will be lower than designed target.

(4) The simulation of the Gamma stochastic process in this paper is based on empirical parameters, and is suitable for predicting resistance degradation in new bridges and the preliminary simulation of resistance in aged bridges. To enhance the accuracy of simulating the resistance evolution behavior in aged bridges, future research will incorporate actual bridge inspection data to dynamically update the model parameters, thus developing a subsequent resistance degradation model of existing bridges that can better conform to the actual situation of box girder bridges.

## Acknowledgement

This research work was jointly supported by the National Natural Science Foundation of China (Grant No. 52208147), Key Laboratory of Damage Diagnosis for Engineering Structures of Hunan Province, Guangdong Provincial Key Laboratory of Intelligent Disaster Prevention and Emergency Technologies for Urban Lifeline Engineering (Grant No. 2022B1212010016).

## Author contribution statement

Meng-Di Yang was responsible for Writing – original draft and Data curation. Xu Zheng was responsible for Conceptualization, Writing – review & editing, and Supervision. Yu Zhou was responsible for Project administration. Ting-Hua Yi was responsible for Resources and Supervision. All authors have approved the final manuscript.

## Data availability

The data that support the findings of this study are available from the corresponding author upon reasonable request.

## Use of AI statement

None.

## Declaration of conflicting interests

The author(s) declared no potential conflicts of interest with respect to the research, authorship and/or publication of this article.

## References

[1] Kumar, R., Cline, D. B. H., Gardoni, P. (2015). A stochastic framework to model deterioration in engineering systems. *Structural Safety*, 53: 36–43.

[2] Jia, G. F., Gardoni, P., Trejo, D., Mazarei, V. (2021). Stochastic modeling of deterioration and time-variant performance of reinforced concrete structures under joint effects of earthquakes, corrosion, and ASR. *Journal of Structural Engineering*, 147(2): 04020314.

[3] Zhang, X. Y., Lu, Z. H., Wu, S. Y., Zhao, Y. G. (2021). An efficient method for time-variant reliability including finite element analysis. *Reliability Engineering & System Safety*, 210: 107534.

[4] Alkaff, A. (2021). Discrete time dynamic reliability modeling for systems with multistate components. *Reliability Engineering & System Safety*, 209: 107462.

[5] Lantsoght, E. O. L. (2024). Assessment of existing concrete bridges by load testing: barriers to code implementation and proposed solutions. *Structure and Infrastructure Engineering*, 20(7-8): 1002–1014.

[6] Cai, C. S., Shahawy, M. (2003). Understanding capacity rating of bridges from load tests. *Practice Periodical on Structural Design and Construction*, 8(4): 209–216.

[7] Faber, M. H., Val, D. V., Stewart, M. G. (2000). Proof load testing for bridge assessment and upgrading. *Engineering Structures*, 22(12): 1677–1689.

[8] Świt, G., Olaszek, P., Casas, J. R. (2012). Proof load testing supported by acoustic emission. An example of application. In Proceedings of Bridge Maitenance, Safety and Life-Cycle Optimization, London, UK, 472–479.

[9] de Vries, R., Lantsoght, E. O. L., Steenbergen, R. D. J. M., Fennis, S. A. A. M. (2024). Time-dependent reliability assessment of existing concrete bridges with varying knowledge levels by proof load testing. *Structure and Infrastructure Engineering*, 20(7-8): 1053–1067.

[10] Chajes, M. J., Shenton III, H. W., Finch, W. W. (2001). Diagnostic and in-service testing of transit railway bridge. *Transportation Research Record*, 1770(1): 51–57.

[11] Duvnjak, I., Bartolac, M., Damjanović, D., Košćak, J. (2020). Performance assessment of a concrete railway bridge by diagnostic load testing. *Structural Concrete*, 21(6): 2363–2376.

[12] Olaszek, P., Łagoda, M., Casas, J. R. (2014). Diagnostic load testing and assessment of existing bridges: examples of application. *Structure and Infrastructure Engineering*, 10(6): 834–842.

[13] Russo, F. M., Wipf, T. J., Klaiber, F. W. (2000). Diagnostic load tests of a prestressed concrete bridge damaged by overheight vehicle impact. *Transportation Research Record*, 1696(1): 103–110.

[14] Mori, Y., Ellingwood, B. R. (1993). Reliability-based service-life assessment of aging concrete structures. *Journal of Structural Engineering*, 119(5): 1600–1621.

[15] Enright, M. P., Frangopol, D. M. (1998). Service-life prediction of deteriorating concrete bridges. *Journal of Structural Engineering*, 124(3): 309–317.

[16] Bhattacharya, B., Li, D., Chajes, M. (2008). Bridge rating using in-service data in the presence of strength deterioration and correlation in load processes. *Structure and Infrastructure Engineering*, 4(3): 237–249.

[17] Xu, X. D., Yu, C. Q., Tang, S. J., Sun, X. Y., Si, X. S., Wu, L. F. (2019). Remaining useful life prediction of lithium-ion batteries based on Wiener processes with considering the relaxation effect. *Energies*, 12(9): 1685.

[18] Xu, X. D., Yu, C. Q., Tang, S. J., Sun, X. Y., Si, X. S., Wu, L. F. (2019). State-of-health estimation for lithium-ion batteries based on wiener process with modeling the relaxation effect. *IEEE Access*, 7: 105186–105201.

[19] Jiang, P. H. (2022). Statistical inference of wiener constant-stress accelerated degradation model with random effects. *Mathematics*, 10(16): 2863.

[20] Yang, Y. M., Peng, J. X., Cai, C. S., Zhou, Y. D., Wang, L., Zhang, J. R. (2022). Time-dependent reliability assessment of aging structures considering stochastic resistance degradation process. *Reliability Engineering & System Safety*, 217: 108105.

[21] Li, Q. W., Wang, C., Ellingwood, B. R. (2015). Time-dependent reliability of aging structures in the presence of non-stationary loads and degradation. *Structural Safety*, 52: 132–141.

[22] Rodríguez-Picón, L. A., Méndez-González, L. C., Pérez-Olguín, I. J. C., Hernández-Hernández, J. I. (2022). A study of the Inverse Gaussian Process with hazard rate functions-based drifts applied to degradation modelling. *Eksploatacja i Niezawodność–Maintenance and Reliability*, 24(3): 590–602.

[23] Peng, W. W., Li, Y. F., Yang, Y. J., Huang, H. Z., Zuo, M. J. (2014). Inverse Gaussian process models for degradation analysis: a Bayesian perspective. *Reliability Engineering & System Safety*, 130: 175–189.

[24] AASHTO (American Association of State Highway and Transportation Officials). (2018). The Manual for Bridge Evaluation, 3rd edn. Farmington Hills: AASHTO.

[25] MoT (Ministry of Transport of the People's Republic of China). (2011). JTG/T J21-2011 Specification for inspection and evaluation of load-bearing capacity of highway bridges. (In Chinese)

[26] Ye, Z. S., Chen, N. (2014). The inverse Gaussian process as a degradation model. *Technometrics*, 56(3): 302–311.

[27] Van Noortwijk, J. M. (2009). A survey of the application of gamma processes in maintenance. *Reliability Engineering & System Safety*, 94(1): 2–21.

[28] Zheng, X., Yi, T. H., Yang, D. H., Li, H. N., Zhou, Y. (2023). Bridge evaluation based on identified influence lines and influence surfaces: multiple-scenario application. *International Journal of Structural Stability and Dynamics*, 23(16-18): 2340026.

[29] MoT (Ministry of Transport of the People's Republic of China). (2018). JTG 3362-2018 Specifications for design of highway reinforced concrete and prestressed concrete bridges and culverts. (In Chinese)

[30] Dieulle, L., Bérenguer, C., Grall, A., Roussignol, M. (2003). Sequential condition-based maintenance scheduling for a deteriorating system. *European Journal of Operational Research*, 150(2): 451–461.

[31] Li, Q. W., Wang, C. (2015). Updating the assessment of resistance and reliability of existing aging bridges with prior service loads. *Journal of Structural Engineering*, 141(12): 04015072.